Characteristics of Ovarian Cancer Immune Cell Invasion and Bioinformatics to Predict the Effect of Immunotherapy

Authors
Lingli Yan[1], Erxi Fan[2], Bin Tan[1]

Affiliations
1 Department of Transfusion Medicine, West China Hospital of Sichuan University, Chengdu, China
2 Department of Ultrasound, Sichuan Provincial People's Hospital, University of Electronic Science and Technology of China, Chengdu, China

Keywords
ovarian cancer, immune cell invasion, TCGA, bioinformatics, immunotherapy

received 04.07.2023
accepted after revision 05.12.2023
published online 19.01.2024

Bibliography
Horm Metab Res 2024; 56: 197–205
DOI 10.1055/a-2231-8475
ISSN 0018-5043

Georg Thieme Verlag, Rüdigerstraße 14, 70469 Stuttgart, Germany

Correspondence
Dr. Bin Tan
West China Hospital of Sichuan University
Department of Transfusion Medicine
Chengdu, China
Tel.: + 8685422523
tanbinhx@163.com

Supplementary Material is available at https://doi.org/10.1055/a-2231-8475

ABSTRACT

Recent studies have confirmed that tumor immune cell infiltration (ICI) is associated with sensitivity of ovarian cancer (OC) immunotherapy and disease progression of OC patients. However, studies related to immune infiltration in OC, has not been elucidated. Two algorithms are used to analyze the OC data in the TCGA and GEO databases. After combining the two data sets, the immune cell content of the sample was estimated by Cell-type Identification By Estimate Relative Subsets of RNA Transcripts (CIBERSORT method). An unsupervised consistent clustering algorithm was used to analyze ICI subtypes and their differentially expressed genes (DEGs). Two subgroups and three ICI gene clusters were identified by unsupervised consensus clustering algorithm. The ICI score was obtained by analyzing the gene characteristics through principal component analysis (PCA). The ICI score ranged from –15.8132 to 18.7211, which was associated with the prognosis of OC patients with immunotherapy. The Toll-like receptor pathway, B-cell receptor pathway, antigen processing and presentation pathway, NK-cell-mediated cytotoxicity pathway, and arginine-proline metabolism pathway were activated in the high ICI score group, suggesting that immune cells in the high ICI score group were activated, thus leading to a better prognosis in this group of patients. Patients with G3–G4 in the high ICI rating group were more sensitive to immunotherapy and had a better prognosis in patients with high tumor mutation burden (TMB). This study suggests that ICI scores can be used as a feasible auxiliary indicator for predicting the prognosis of patients with OC.

ABBREVIATIONS

TCGA	The Cancer Genome Atlas
OS	Overall survival
ICI	Immune cell infiltration
OC	Ovarian cancer
CIBERSORT	Cell-type Identification By Estimating Relative Subsets Of RNA Transcripts
DEGs	Differentially expressed genes
PD-L1	Programmed death ligand-1
PD-1	Programmed death-1
TMB	Tumor mutation burden
TME	Tumor microenvironment
NGS	Next-generation sequencing
FPKM	Fragments per kilobase million
TPM	Kilobase million
CDF	Cumulative distribution function

Background

Ovarian cancer (OC) is one of the three most common gynecological malignancies worldwide. The clinical symptoms of early OC are not obvious, and it is difficult to diagnose. Most of these are already in an advanced stage at the time of diagnosis. Their five-year overall survival rate is only approximately 40 to 45 % [1], of which it is only 20–30 % for advanced patients [2]. At present, the main method of treatment is surgery combined with radiotherapy and chemotherapy. However, some patients experience drug resistance and recurrence after taking chemotherapy drugs such as cisplatin leading to a poor prognosis [3].

Tumor immunotherapy is an antitumor therapy based on immunotherapy, which has become a research highlight in tumor therapy. It achieves antitumor effects by activating and enhancing the ability of the immune system to recognize and eliminate tumor cells and mobilize autoimmunity [4, 5]. Between them, programmed death ligand-1 (PD-L1), as a membrane inhibiting molecule on the surface of tumor cells, can restrict T cells by activating the PD-1/PD-L1 inhibitory signaling pathway. It creates an immunological microenvironment that favors the growth of tumor cell growth and induces immune escape from tumors. Checkpoint inhibitor therapy targeting programmed death-1 (PD-1)/PD-L1 can block this pathway, restore immune activity of T cells, enhance the immune response and improve the immune system response to tumor cells with its ability to recognize and kill tumor cells. This therapy has achieved remarkable results in the treatment of various solid tumors. Numerous studies have confirmed that immune checkpoint inhibitors have some effect in patients with early-stage OC patients [6, 7]. However, the treatment effect in advanced patients is not satisfactory [8, 9]. Tumor mutation burden (TMB) is an immunophenotypic marker that describes the number of non-synonymous mutations in a tumor sample. This represents the degree of genomic instability and the probability of neoepitopes appearing on the cell surface [10]. TMB can be used as an independent predictor of the PD-1/PD-L1 treatment effect, and the effectiveness of immune checkpoint inhibitors can be predicted by screening suitable biomarkers in order to filter the effective patient population for this method [11]. However, no study has shown an association between TMB and the response to immunotherapy in OC.

Solid tumors can escape the surveillance of the immune system through various mechanisms of immune evasion or resistance, creating an environment suitable for their growth – the tumor microenvironment (TME) [12]. TME leads to the dysfunction of immune cells such as T cells and NK cells, inhibits the activation of antigen-presenting cells and promotes the formation of microvascular beds and matrix barriers, inducing the formation of immunosuppressive effects and causing tumor immune escape [13]. Correspondingly, the expression of tumor self-stimulatory molecules (CTLA-4 and PD-1/PDL-1) is also downregulated, allowing tumor cells to prevent T cells from being killed [14]. It is important to elucidate the TME of OCs from the functional perspective of immune cells by establishing an antitumor response of immune cells to prevent occurrence, progression or recurrence of tumors. Among them, immune cells, metabolic pathways, and intracellular signaling molecules represent unique properties of the TME and have also become important indicators of immunotherapeutic response and prognosis [15].

Next-generation sequencing (NGS) technology, also known as high-throughput sequencing technology, breaks DNA molecules into short fragments of 500 to 800 bp and simultaneously sequences tens of millions or even hundreds of millions of DNA fragments on the same chip [16]. With the advancement of NGS, gene expression profiling has become an effective method for identifying differentially expressed genes in various diseases, thereby contributing to the study of pathogenesis and the development of new biomarkers [17]. NGS-related algorithms are also being successively updated. CIBERSORT is an analytical tool that uses microarray data or RNA sequencing data to assess the expression of immune cells in a sample and obtain different proportions of immune cells [18]. The ESTIMATE algorithm is used to describe the ratio of stromal cells to immune cells in a tumor. This is an algorithm that can predict tumor purity and the ratio of stromal cells to immune cells in tumor tissue [19].

The OC response to immunotherapy is limited. However, targeted therapy-sensitive/resistant subgroup analysis based on tumor biomarker stratification may help improve the predictive power of response to immunotherapy. These biomarkers mainly include PD-1/PD-L1, TMB, ICI, etc. To find a biomarker that predicts sensitivity to immunotherapy, we analyzed the gene expression profiles of multiple tumor samples from the TCGA and GEO databases using bioinformatics analysis combined with the CIBERSORT and ESTIMATE algorithms, building a framework that can accurately predict OC patients' prognosis and response to immunotherapy.

Materials and Methods

Data collection and processing

The OC patients RNA dataset [fragments per kilobase million (FPKM)] and the corresponding clinical data and SNP data were obtained from the TCGA database (https://portal.gdc.cancer.gov), and GSE140082 microarray sequencing data were obtained from the Gene Expression Omnibus (GEO) database (https://www.ncbi.nlm.nih.gov/geo/). We converted the TCGA data to a transcripts per kilobase million (TPM) matrix because the expression profile (FPKM value) data of the TCGA OC dataset are different from the microarray sequencing data [20]. The two expression datasets were combined for further analysis using the limma and sav packages provided by BiocManager.

Consensus clustering of immune cell infiltration

CIBERSORT is an algorithm for deconvoluting the expression matrix of human immune cell subtypes based on the principle of linear support vector regression. For microarray expression matrices and sequencing expression matrices, deconvolution analysis of unknown mixtures and expression matrices containing similar cell types outperforms other methods. The algorithm provides a default set of gene expression signatures for 22 immune cell subtypes [18]. ESTIMATE is an algorithm that can estimate the stromal score and immune score of tumor samples from expression data and can be used to estimate tumor purity. The CIBERSORT algorithm was used to estimate the proportion of immune cells in samples from OC patients, and the ESTIMATE algorithm was used to calculate stromal and immune scores. The Consensus-ClusterPlus R package

was used to perform unsupervised consensus clustering analyzes based on the ICI pattern of each ovarian cancer sample [21].

Differentially expressed genes (DEGs) associated with the ICI phenotype

This unsupervised consensus clustering algorithm was used to classify patients into different ICI subgroups based on the content of immune cells in the OC samples. The process was to extract a dataset with a certain sample size by resampling and filter out the optimal K-value. The rationality principal component analysis (PCA) algorithm was calculated the number of different clusters [22]. The K-value is equal to the number of groups. The selection principle of the optimal K-value is as follows: (1) The cumulative distribution function (CDF) value is small, and the growth of it is slow; (2) There are no small clusters or cross-clusters between different subtypes; and (3) The intracluster correlation is high. Using this algorithm, patients were divided into different ICI subgroups, and each subgroup represented a different degree of tumor immune cell infiltration. A false discovery rate < 0.05 and absolute fold change < 1 were taken as criteria.

ICI score dimensionality reduction and generation

We performed unsupervised consensus clustering on all DEGs again to obtain the optimal number of subgroups and then divided clusters according to this number. The DEG values that were positively or negatively correlated with these clusters were taken as ICI gene signatures A and B, and the dimensionality reduction of ICI gene signatures A and B is (was) performed using the Boruta algorithm [23]. PCA extracts principal components as feature scores, where PC1A represents the first component of signature A and PC1B represents the first component of signature B. Finally, we used a method similar to the Gene Expression Grading Index. The ICI score of each patient was determined using the Boruta package according to Equation 1: ICI score = ΣPC1A – ΣPC1B [24].

Analysis and processing of mutation data

Mutation data on OC patients were downloaded from the TCGA database (https://portal.gdc.cancer.gov) to determine the mutational burden of OCs. We counted the total number of asynchronous mutations in OC and assessed somatic changes in OC driver genes to determine ICI scores. The driver genes of OC were identified using the "maftool" software package [25]. The top 20 driver genes with the highest mutation frequency are displayed.

Statistical analysis of data

Statistical analysis in this study was performed using R version 4.2.0 software. The Kruskal–Wallis test was used to compare the differences between more than two groups, and the Wilcoxon test was used to compare the differences between the two groups. Find the best cutoff value using X-tile software. The rationale of it is to use different values as cutoffs for statistical tests. The result with the smallest p-value can be considered the best cutoff value [24]. A Kaplan–Meier plotter was used to generate subgroup survival curves for each dataset. The log-rank test was used to assess significant differences between subgroups. Two-tailed $p < 0.05$ was considered statistically significant.

Results

Situation of immune cell infiltration in the OC TME

Combining 761 samples from two databases (array expression datasets: GSE140082 and TCGA) into one set, immune cell levels in OC tissues were quantified using CIBERSORT and ESTIMATE algorithms. Information about the data set can be found in ▶ **Table 1**. All metacohort samples were found to be systematically clustered by CIBERSORT. Empirical cumulative distribution function plots and delta area plots to represent the results of consistent clustering, where K is the number of subgroups. When plotting these two graphs to analyze the optimal K-value for sample distribution stability, we chose K = 2 as the optimal number of clusters, as shown in ▶ **Fig. 1a**. ▶ **Fig. 1b** shows the expression heatmap of the correlation clustering results. The overall survival rates for the 2 independent ICI subtypes were significantly different (log-rank test, $p < 0.05$), and the results showed that patients from ICI cluster A had a better prognosis than patients from ICI cluster B (▶ **Fig. 1c**). We found that the expression of PD-1 and PD-L1, two important immune checkpoints, was lower in ICI cluster B than in A cluster (▶ **Fig. 1d, e**). We further defined the intrinsic biological differences leading to different clinical subtypes by comparing the composition of immune cells in the TME, as shown in ▶ **Fig. 1f** in ICI cluster A with B: naive B cells, memory B cells, plasma cells, CD8 T cells, CD8 T cells, CD4 memory-activated T cells, follicular helper T cells, γδT cells, M1 macrophages, M2 macrophages, and resting mast cells having the highest levels. ICI cluster B had the highest levels of CD4 memory resting T cells, resting NK cells, M0 macrophages, and activated mast cells. The immune score of ICI cluster A was significantly higher than that of ICI cluster B (p^{***}), indicating a higher percentage of immune cells. The results in ▶ **Fig. 1g** show the correlation of 22 types of immune cells.

▶ **Table 1** Data sets.

Record	Platform	Country	Year	Number of normal samples	Number of OV samples
TCGA	Illumina HiSeq	USA	2022	0	381
GSE140082	GPL14951 Illumina HumanHT-12 WG-DASL V4.0 R2 expression beadchip	USA	2019	0	380

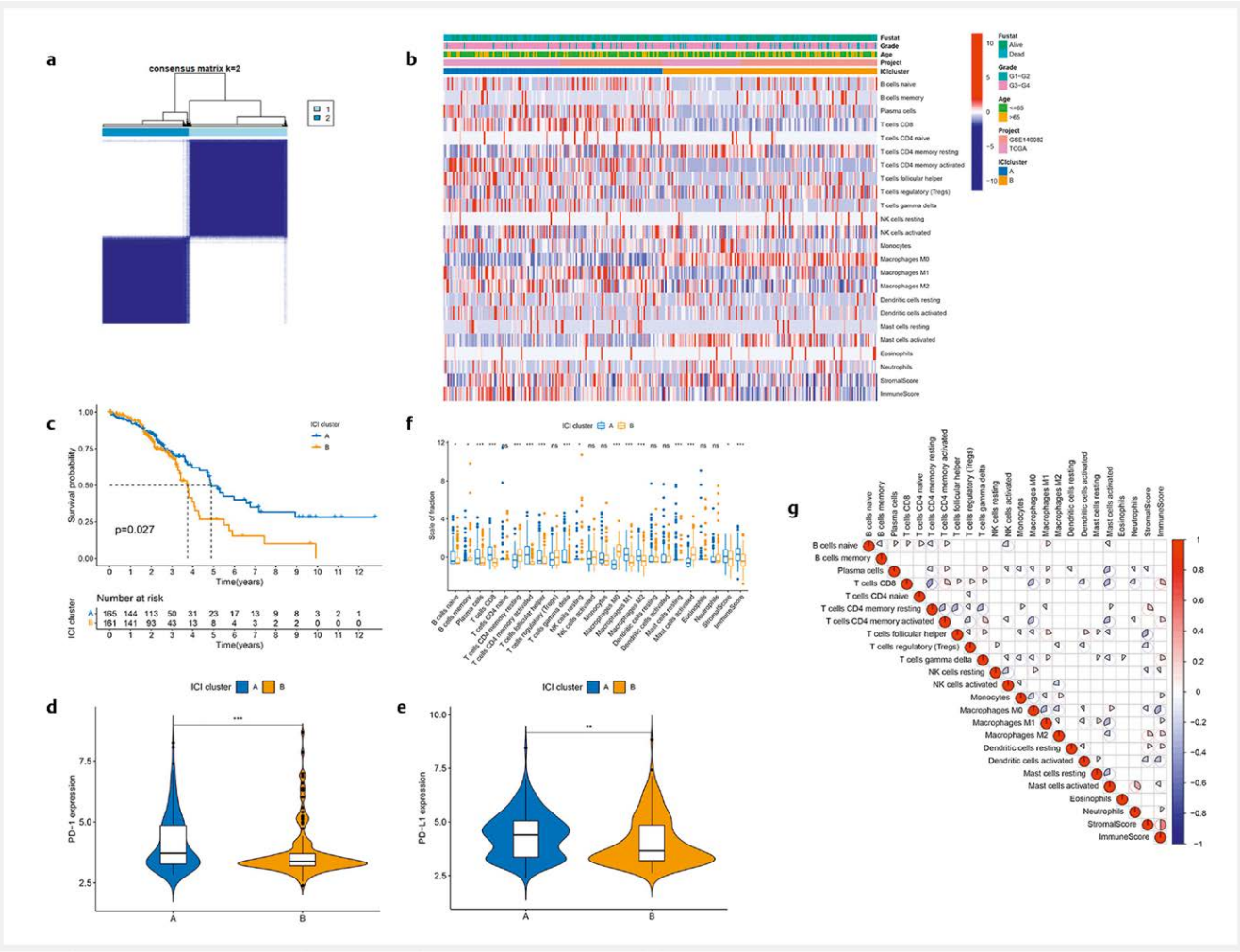

▶ **Fig. 1** Landscape of ICI in the TME of OC. **a**: Consensus clustering was used to divide these samples into 2 ICI subgroups in accordance with the content of immune cells in these samples. **b**: Heatmap of the tumor-infiltrating immune cells in four independent OC cohorts. Rows indicate tumor-infiltrating immune cells, and columns indicate the OC samples. The color intensity value indicates the fraction of different immune cells. **c**: Kaplan–Meier survival analysis for overall survival (OS) of all OC patients from three ICI clusters. PD-1 (**d**) and PDL-1 (**e**) expression among different ICI clusters. **f**: The difference in the tumor-infiltrating immune cell types between the different ICI clusters. **g**: The proportion and correlation of tumor-infiltrating immune cells in the three ICI clusters. *p<0.05. **p<0.01. ***p<0.001. ****p<0.0001.

DEGs of immune gene subtypes

We also performed differential immunophenotyping analyses. The gene expression levels of all samples were obtained by performing DEGs analysis, and after correcting the p-value, unsupervised consistent clustering analysis was performed according to DEGs, and obtained 3 gene clusters (▶ **Fig. 2a**). Subsequently, survival curves of different sample types and genotypes were drawn. We found that the patients from the C gene cluster had the best prognosis, while the patients from the B gene cluster had the worst prognosis. The prognosis of the 3 groups was significantly different for each genotype (p***) (▶ **Fig. 2b**). Analysis of differences between immune cells by genotype is shown in ▶ **Fig. 2c**. Gene cluster A had higher levels of M2-type macrophages. Gene cluster B has CD4 memory resting T cells, resting NK cells, M0 macrophages, activated dendritic cells, and activated mast cells, and the C gene cluster had a higher proportion of plasma cells, CD8 + T cells, activated CD4 + memory T cells, γδT cells, M1 macrophages, and resting dendritic cells. There was no significant difference in the effects of the three gene clusters on naive B cells, memory B cells, naive CT4 + T cells, T helper follicular cells, Tregs, activated NK cells, monocytes, resting mast cells and neutrophil learning differences. Furthermore, the C gene cluster had the highest immune and stromal scores, while the B gene cluster had the lowest immune and stromal scores. PD-1 and PD-L1 were highly expressed in the C gene cluster, followed by the A gene cluster and the B gene cluster (▶ **Fig. 2d, e**). The correlation between gene expression and typing was shown in ▶ **Fig. 2f**. If the correlation was positive, it was divided into group A, while if the correlation was negative, it was divided into group B.

Correlation between ICI scores and immune checkpoint signals

Genomes samples A and B were evaluated separately using the PCA algorithm. The final score of each sample was obtained from the score of group A minus the score of group B (**Supplementary Table 1S**). Pa-

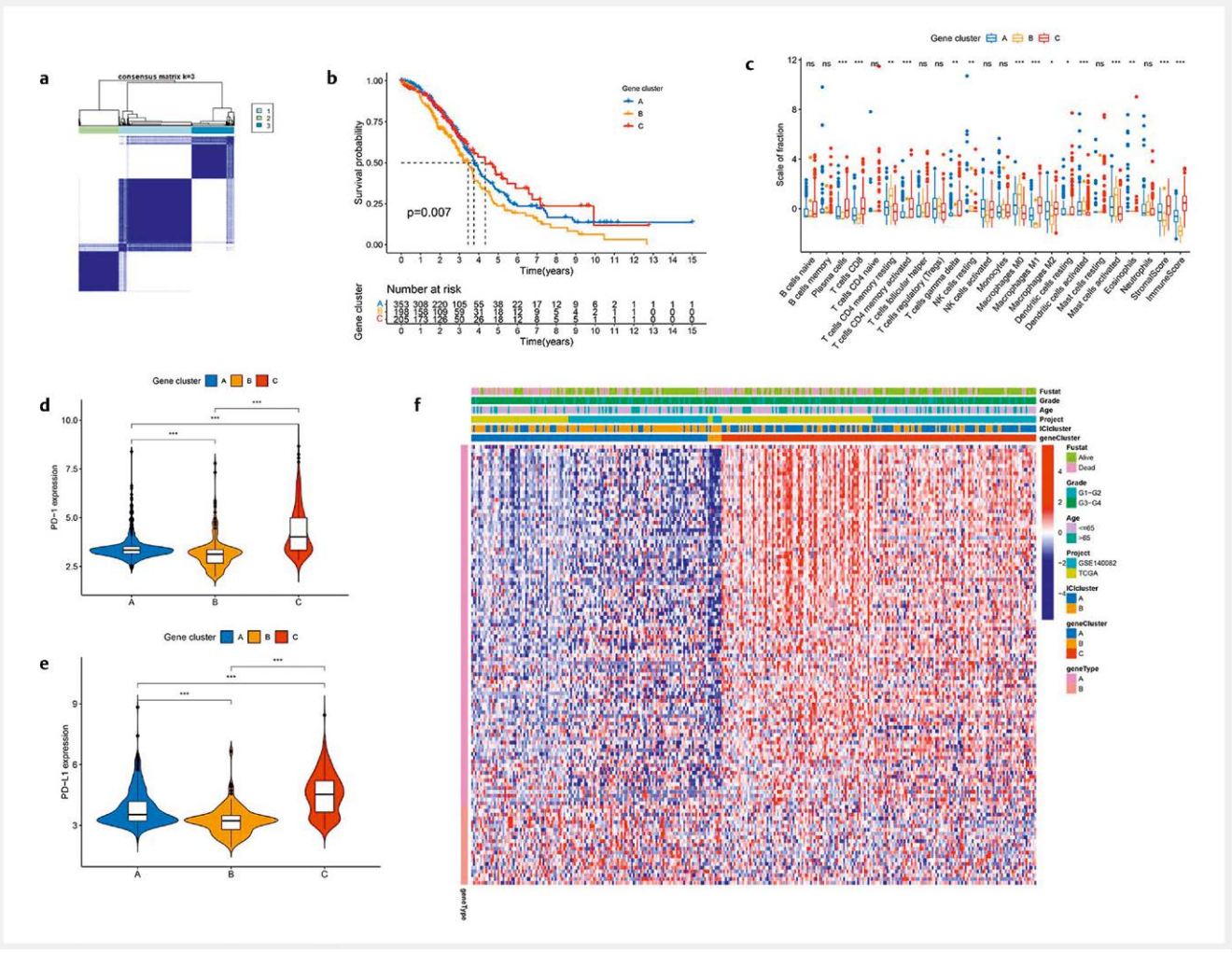

▶ **Fig. 2** An Immunophenotyping differential analysis. **a**: After differential analysis of all genes, the expression of a gene in all samples and the corrected p value are obtained, and then the samples are typed according to the differential genes, which are divided into 3 types here. **b**: Kaplan–Meier curves for the OS of the three groups of patients. **c**: Analysis of genetic types of immune cell differences. The horizontal coordinates are the names of immune cells. The vertical coordinate is the content of immune cells. **d**, **e**: Differences in PD1 and PD-L1 expression among different ICI gene clusters. **f**: The genetic typical hot diagram, the horizontal coordinates are samples, the vertical coordinates are gene expression, the genetic expression and the classification are positively correlated and divided into group A, and negative correlations are divided into group B.

tients were divided into high and low scoring groups based on the selected optimal cutoff. The distribution of clinical information related the OC among the 3 gene clusters is shown in ▶ **Fig. 3a**. CD274, CTLA4, PDCD1, HAVCR2, IDO1, and LAG3 are immune checkpoint-related signals. By selecting CD8A, CXCL10, CXCL9, GZMA, GZMB, IFNG, PRF1, TBX2, and TNF as signals associated with immune activity, we compared the expression of these genes in the low and high ICI score groups (▶ **Fig. 3b**) to assess immune activity and tolerance. The results showed that all genes except TBX2 were significantly overexpressed in patients with high ICI scores (p***). In addition, gene set enrichment analysis revealed that the TOLL-like receptor pathway, B-cell receptor pathway, antigen processing and presentation pathway, NK-cell-mediated cytotoxicity pathway, and arginine-proline metabolism pathway were significantly associated with high ICI scores. All pathways were not significantly enriched in the low-scoring group (▶ **Fig. 3c**). In the metacohort, patients with high ICI scores had a better prognosis than patients with low ICI scores (▶ **Fig. 3d**). This result was statistically different in the survival analysis from GSE140082 (▶ **Fig. 3e**) and TCGA database (▶ **Fig. 3f**).

ICI scores combined with tumor mutation burden (TMB) was used as a predictor of prognosis in OC patients

TMB may predict the outcome of immunotherapy in patients with advanced cancer. The results of Spearman correlation analysis showed that there was no significant difference between the ICI score and TMB correlation analysis (Spearman coefficient: R = 0.043, p = 0.5, ▶ **Fig. 4a**). We divided the patients into a high TMB group and a low TMB group according to the best cutoff value and analyzed the survival of patients in the high TMB group and the low TMB group. However, we found that the TMB level was significantly associated with prognosis (p***) (▶ **Fig. 4b**). The results of TMB subgroup analysis showed that patients with high ICI scores had a better prognosis than patients with high TMB, while patients with low TMB and ICI

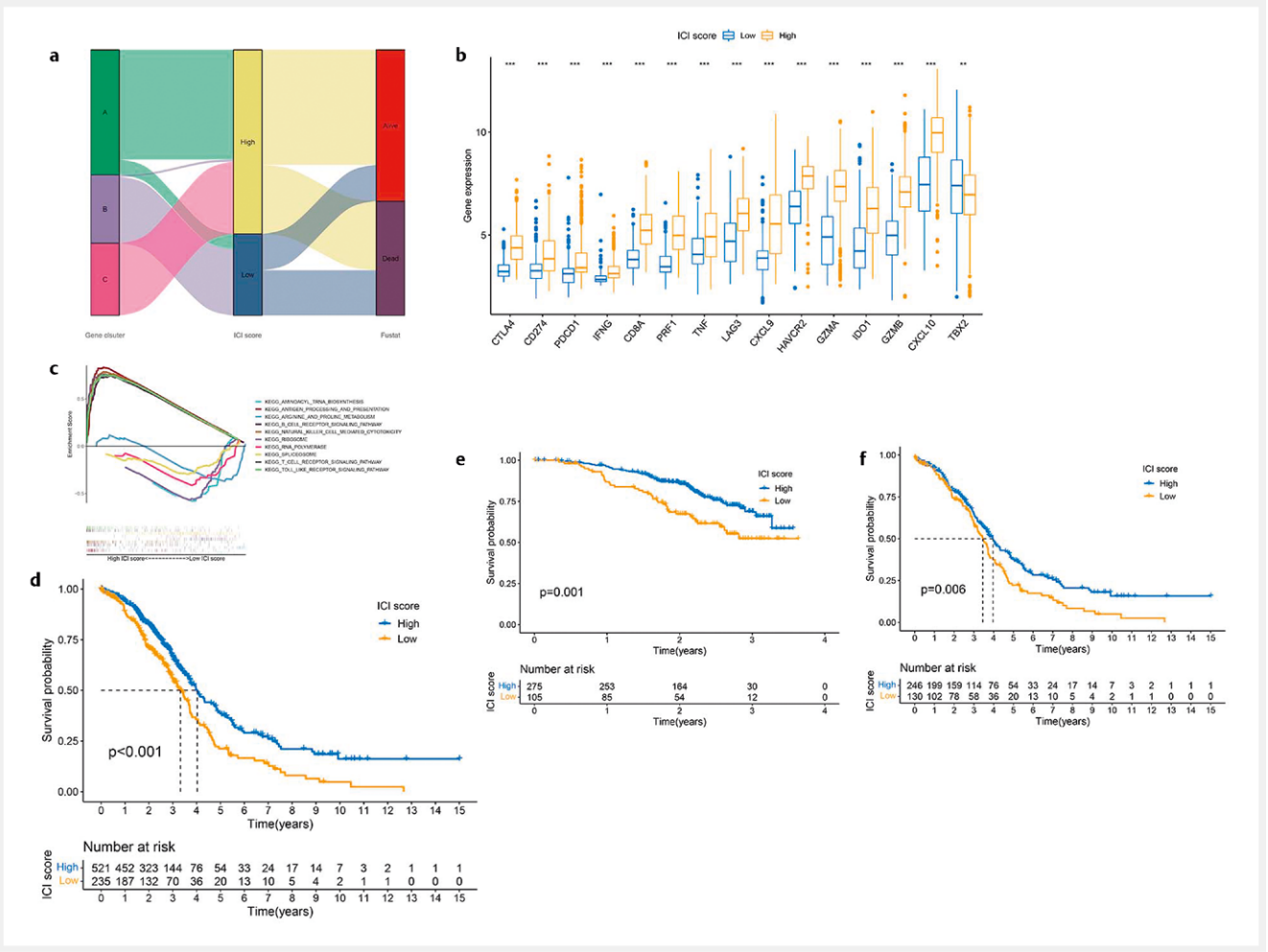

▶ **Fig. 3** **a**: Alluvial diagram of ICI gene cluster distribution in groups with different ICI clusters. ICI scores, and survival outcomes. **b**: The difference between the immune checkpoint-relevant genes (CD274, CTLA4, PDCD1, HAVCR2, IDO1, LAG3) and immune activation-relevant genes (CD8A, CXCL10, CXCL9, GZMA, GZMB, IFNG, PRF1, TBX2, TNF) expressed in the high and low ICI score subgroups. **c**: GSEA results of high and low ICI score subgroups. **d**: Kaplan–Meier curves for high and low ICI score groups in the meta-cohort. **e** and **f** represent Kaplan–Meier curves of groups with high and low ICI scores in GSE140082 and TCGA metacohort, respectively.

scores had a poor prognosis (▶ **Fig. 4c**). ▶ **Fig. 4d, e** showed that we further analyzed the distribution of somatic variants in OC driver genes between subgroups with high and low ICI score subgroups. The top 20 driver genes with the highest mutation rates are displayed. Aside from that, we also found that the expression of USH2A was significantly different between the high and low ICI score groups ($p < 0.05$). These results suggest that the ICI score can serve as an effective predictor and can be combined with the TMB to provide a new approach to study tumor ICI composition and the mechanisms of actions of gene mutations in cancer immunotherapy.

Correlation analysis between ICI scores and survival status of patients

A correlation analysis between ICI scores and clinical outcome was performed. In the TCGA and GSE140082 cohorts, a higher proportion of patients with high ICI scores survived than those with low ICI scores (▶ **Fig 5a**). Furthermore, patients who survived had higher ICI scores (▶ **Fig. 5b**). Survival analysis of clinical groups showed that the ICI scores was significantly correlated with the prognosis of patients with OC grades 3–4, indicating that the ICI score was suitable for patients with high grade (▶ **Fig. 5c**).

Discussion

The mechanism of OC and immunity has received considerable attention [7–9, 26]. It has important clinical value in immunotherapy because the pathogenesis of OC is very complicated and involves a variety of factors, such as gene mutations, endocrine changes, and microbial infections [27–29]. Previous studies have established a transcription-factor-related prognostic model for OC by consistent cluster analysis and found significant differences between the risk score and the responsiveness of OC patients to immune checkpoint inhibitor therapy [30]. Therefore, a better elucidation of the interaction between tumor cells and immune cells and the molecular mechanisms may provide new targets for immunotherapy in ovarian cancer patients. We merged the OC dataset in the TCGA

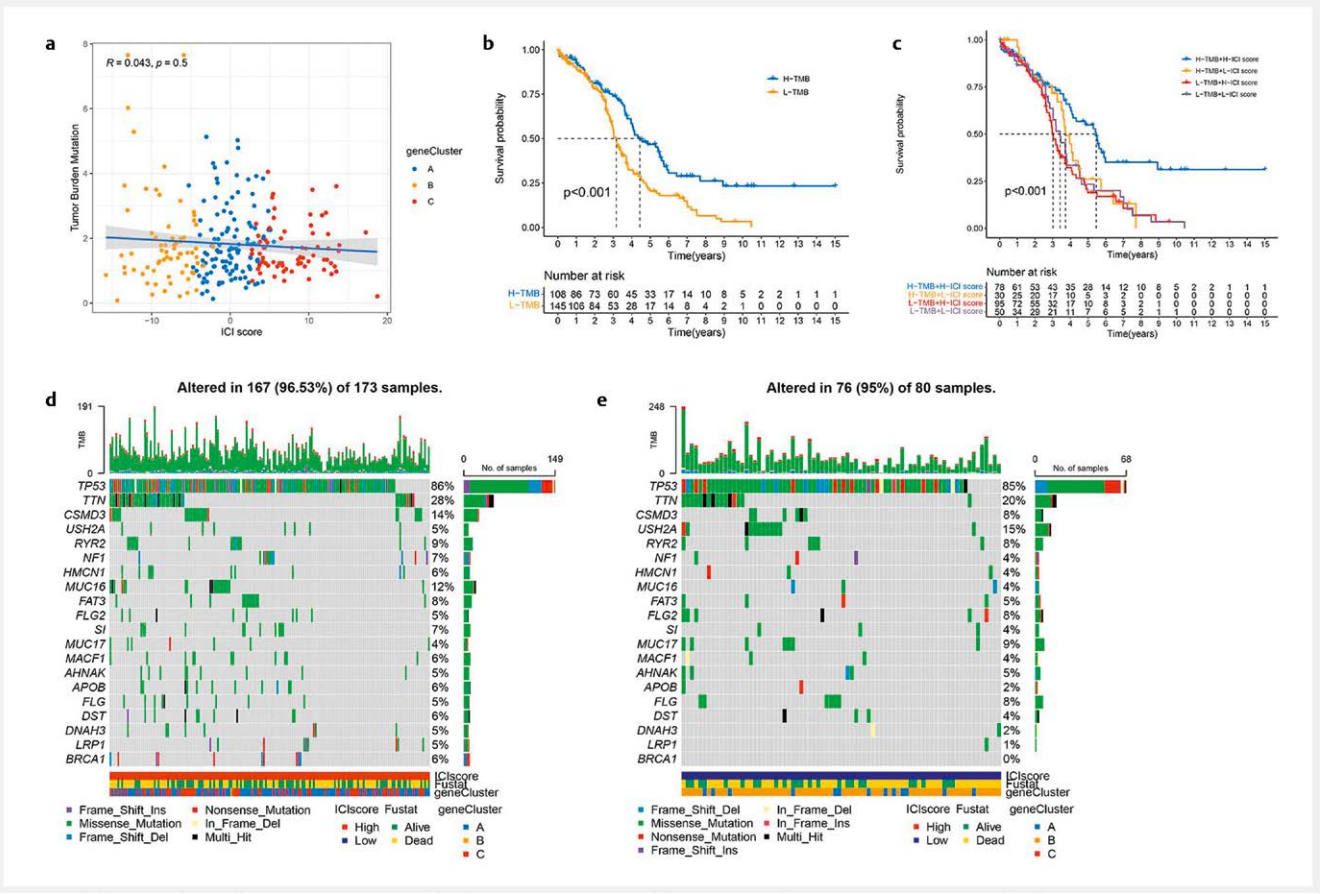

▶ **Fig. 4** **a**: Scatter plot used to describe the correlation between the ICI score and mutation load in the meta-cohort. **b**: Kaplan–Meier curves for the high and low TMB groups of the meta-cohort. **c**: Kaplan–Meier curves for patients in the meta-cohort stratified by both TMB and ICI scores. **d**: Heatmap of somatic variants for high ICI scores. **e**: Heatmap of somatic variants for low ICI scores.

and GEO databases and estimated the immune cells content of each sample using the CIBERSORT algorithm. By unsupervised consistent cluster analysis. Two ICI subgroups were obtained, and the subgroup was analyzed for differences in gene expression, obtaining 3 ICI gene clusters. Finally, the ICI score was determined by genetic symbol analysis using through PCA. The group with high ICI score had a good prognosis, which may be related to the TOLL-like body pathway, B-cell receptor pathway, antigening and presence pathway, NK-cell-mediated cytotoxic pathway, and arginine-proline metabolic pathway. In addition, patients with high ICI score are more sensitive to immunotherapy, and patients with high ICI scores and high TMB have a better prognosis. This means that the higher the immune score, the better the future. After analyzing the DEGs of different ICI subgroups, it was found that different ICI gene clusters were also associated with patient prognosis. In conclusion, ICI score was related to the patient's prognosis and the sensitivity of immunotherapy according to scoring the ICI and grouping. Our studies showed that 14 immune checkpoints and immune activation-related genes had high expression among OC patients with high ICI scores.

The ICI mode requires individualized treatment due to different individual immune environments. Tumor subtype-specific biomarkers have been uesd to predict the prognosis of malignancies such as breast cancer, bladder cancer, and pancreatic cancer [31–33]. The GSEA results showed that immune-related signaling pathways were activated in the high ICI ratings score group, but not in the low ICI scores group. For patients with higher grade, the prognosis of high ICI rating score group patients were significantly better than that of the low ICI score group patients. Activation of these pathways is associated with the treatment of OC.

The TMB describes the number of nonsynonymous mutations in tumor samples and represents the degree of the unstable genome and the possibility of new surface positions on the cell surface. Under normal circumstances, TMB is divided into two types, high and low, of which TMB is defined as Megabase [34]. High TMB phenotypes represent a large number of mutant proteins expressed on the cell surface in the form of new surfaces [35]. In physical tumor studies, TMB high surface types can predict the response to ICI related immune treatment [36]. However, OC has always been considered a "cold tumor" with low TMB. Numerous studies have confirmed that the sensitivity of OC to immunotherapy has no significant association with TMB. TMB cannot be used as an independent indicator to predict the sensitivity of OC treatment [34]. However, some studies have confirmed that TMB can be used in combination with PDL-1 expression level to predict immunotherapy sensitivity of OC patients. High expression of PD-1/PD-L1 can

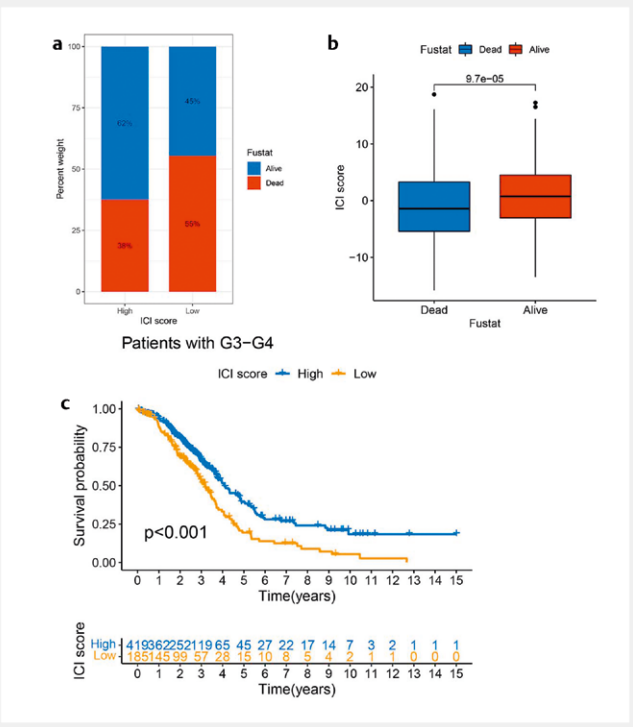

▶ **Fig. 5** Correlation analysis between ICI scores and survival status of patients. **a**: The percent weight of the ICI scores and the proportion of survival/death of patients. **b**: The correlation analysis between the ICI scores and patients' Fustat. **c**: Kaplan–Meier curves for G3-G4 OC patients with high and low ICI scores.

predict the response to immunotherapy independently of TMB status, but the combination of the two biomarkers is better than either one alone [36]. The results of our study indicated that although the expression level of TMB does not have a significant relationship with the prognosis of patients, the prognosis in high ICI score groups in patients with high TMB patients is better than the lower TMB group. It is concluded that ICI score and TMB might play a role in different aspects of OC immunotherapy, and ICI score can be used as a feasible auxiliary indicator to predict the prognosis of TMB patients with different states.

These studies are limited to research data coming from the database, and there are no experimental data to support the results. Therefore, while we need to further expand the research samples, combine laboratory results to confirm the results of our study, and further investigate the significance of the ICI score for clinical patients undergoing immunotherapy, we need to conduct corresponding studies on the intrinsic regulatory mechanism.

Acknowledgement

Lingli Yan conceived and designed the study, draw the charts and wrote the paper. Erxi Fan and Bin Tan provided the critical revision. All authors read and approved the manuscript. We sincerely thank TCGA and GEO for sharing the huge amount of data.

Funding Information

Sichuan Science and Technology Program No.2022NSFSC1513.

Conflict of Interest

The authors declare that they have no conflict of interest.

References

[1] Henderson JT, Webber EM, Sawaya GF. Screening for ovarian cancer: updated evidence report and systematic review for the US preventive services task force. JAMA 2018; 319: 595–606

[2] Reid BM, Permuth JB, Sellers TA. Epidemiology of ovarian cancer: a review. Cancer Biol Med 2017; 14: 9–32

[3] Alison EF, Jessica AB, Elizabeth LC et al. Mechanisms of drug resistance in high-grade serous ovarian cancer. Hematol Oncol Clin North Am 2018; 32: 983–996

[4] Saleh R, Elkord E. Acquired resistance to cancer immunotherapy: Role of tumor-mediated immunosuppression. Semin Cancer Biol 2020; 65: 13–27

[5] Sanmamed MF, Chen L. A Paradigm shift in cancer immunotherapy: from enhancement to normalization. Cell 2019; 176: 677

[6] Liu JF, Gordon M, Veneris J et al. Safety, clinical activity and biomarker assessments of atezolizumab from a Phase I study in advanced/recurrent ovarian and uterine cancers. Gynecol Oncol 2019; 154: 314–322

[7] Disis ML, Taylor MH, Kelly K et al. Efficacy and safety of Avelumab for patients with recurrent or refractory ovarian cancer: phase 1b results from the JAVELIN solid tumor trial. JAMA Oncol 2019; 5: 393–401

[8] Matulonis UA, Shapira-Frommer R, Santin AD et al. Antitumor activity and safety of pembrolizumab in patients with advanced recurrent ovarian cancer: results from the phase II KEYNOTE-100 study. Ann Oncol 2019; 30: 1080–1087

[9] Odunsi K. Immunotherapy in ovarian cancer. Ann Oncol 2017; 28: viii1–viii7

[10] Choucair K, Morand S, Stanbery L et al. TMB: a promising immune-response biomarker, and potential spearhead in advancing targeted therapy trials. Cancer Gene Ther 2020; 27: 841–853

[11] Papaioannou NE, Beniata OV, Vitsos P et al. Harnessing the immune system to improve cancer therapy. Ann Transl Med 2016; 4: 261

[12] Dominique CH, Lalita AS. The Tumor microenvironment innately modulates cancer progression. Cancer Res 2019; 79: 4557–4566

[13] Xian JJ, Jie W, Xiang YD et al. Role of the tumor microenvironment in PD-L1/PD-1-mediated tumor immune escape. Mol Cancer 2019; 18: 10

[14] Keenan TE, Burke KP, Van AE. Genomic correlates of response to immune checkpoint blockade. Nat Med 2019; 25: 389–402

[15] Drakes ML, Stiff PJ. Regulation of ovarian cancer prognosis by immune cells in the tumor microenvironment. Cancers (Basel) 2018; 10: 302

[16] Rick K, Rita DB, Bianca JB et al. Sequencing in oncology: genetic diagnosis, risk prediction and cancer classification. Int J Mol Sci 2017; 18: 308

[17] Ming C, Hong YZ. Next-generation sequencing in liquid biopsy: cancer screening and early detection. Hum Genomics 2019; 13: 34

[18] Newman AM, Liu CL, Green MR et al. Robust enumeration of cell subsets from tissue expression profiles. Nat Methods 2015; 12: 453–457

[19] Yoshihara K, Shahmoradgoli M, Martínez E et al. Inferring tumour purity and stromal and immune cell admixture from expression data. Nat Commun 2013; 4: 2612

[20] Wagner GP, Kin K, Lynch VJ. Measurement of mRNA abundance using RNA-seq data: RPKM measure is inconsistent among samples. Theory Biosci 2012; 131: 281–285

[21] Yu G, Wang LG, Han Y et al. ClusterProfiler: an R package for comparing biological themes among gene clusters. OMICS 2012; 16: 284–287

[22] David CC, Jacobs DJ. Principal component analysis: a method for determining the essential dynamics of proteins [J]. Meth Mol Biol (Clifton, N.J.) 2014; 1084: 193–226

[23] Kursa MB, Rudnicki WR. Feature selection with the Boruta package. J Stat Softw 2010; 36: 1–13

[24] Sotiriou C, Wirapati P, Loi S et al. Gene expression profiling in breast cancer: understanding the molecular basis of histologic grade to improve prognosis. J Natl Cancer Inst 2006; 98: 262–272

[25] Mayakonda A, Lin DC, Assenov Y et al. Maftools: efficient and comprehensive analysis of somatic variants in cancer. Genome Res 2018; 28: 1747–1756

[26] Fernanda GH, Melita I, Lana EK et al. Rational combinations of immunotherapy with radiotherapy in ovarian cancer. Lancet Oncol 2019; 20: e417–e433

[27] Basheerulla S, Tabassum Z, Krishnan B et al. An overview of ovarian cancer: molecular processes involved and development of target-based chemotherapeutics. Curr Top Med Chem 2021; 21: 329–346

[28] Carsten G, Günter E. Role of gonadotropin-releasing hormone (GnRH) in ovarian cancer. Cells 2021; 10: 437

[29] Huiyan C, Zhichao W, Lifeng C et al. Opportunities and challenges of the human microbiome in ovarian cancer. Front Oncol 2020 10: 163. eCollection 2020

[30] Li H, Wu N, Liu ZY et al. Development of a novel transcription factors-related prognostic signature for serous ovarian cancer. Sci Rep 2021; 11: 7207

[31] Zhao S, Ma D, Xiao Y et al. Molecular subtyping of triple-negative breast cancers by immunohistochemistry: molecular basis and clinical relevance. Oncologist 2020; 25: e1481–e1491

[32] Efstathiou JA, Mouw KW, Gibb EA et al. Impact of immune and stromal infiltration on outcomes following bladder-sparing trimodality therapy for muscle-invasive bladder cancer. Eur Urol 2019; 76: 59–68

[33] Collisson EA, Bailey P, Chang DK et al. Molecular subtypes of pancreatic cancer. Nat Rev Gastroenterol Hepatol 2019; 16: 207–220

[34] Choucair K, Morand S, Stanbery L et al. Nemunaitis, J. TMB: a promising immune-response biomarker, and potential spearhead in advancing targeted therapy trials. Cancer Gene Ther 2020; 27: 841–853

[35] Yarchoan M, Hopkins A, Jaffee EM. Tumor mutational burden and response rate to PD-1 inhibition. N Engl J Med 2017; 377: 2500–2501

[36] Yarchoan M, Albacker LA, Hopkins AC et al. PD-L1 expression and tumor mutational burden are independent biomarkers in most cancers. JCI Insight 2019; 4: e126908